

Study of Neutron-Induced Reactions on He^3 at $E_n = 14.4$ MeV

B. ANTOLKOVIĆ, G. PAIĆ, P. TOMAŠ, AND D. RENDIĆ

Institute "Ruđer Bošković," Zagreb, Yugoslavia

(Received 13 March 1967)

Angular distributions of the $\text{He}^3(n,d)\text{D}$ and $\text{He}^3(n,p)\text{T}$ processes with 14.4-MeV neutrons have been measured using a gas He^3 target and a counter-telescope system. The differential cross sections for elastic scattering, $\text{He}^3(n,n)\text{He}^3$, have been obtained by the same technique, detecting recoil He^3 particles in the range from 0° to 40° (lab). The theoretical analysis of the data has been made within the framework of existing theories. The Legendre-polynomial-expansion curves fitted to the data are also presented.

INTRODUCTION

THE measurement of neutron-induced reactions on He^3 offers the possibility of investigating reaction mechanisms and interactions in a system of four nucleons, i.e., two protons and two neutrons. The processes which can be measured are:

(1) Elastic scattering. The analysis of experimental data involves the knowledge of the wave functions of He^3 and the $n\text{-He}^3$ system as well as the knowledge of the interaction between the nucleons. Thus the theoretical analysis of this process can be a test for the data known from other experiments, e.g., electron scattering, photodisintegration, etc.

(2) Reactions in which two particles are produced in the final channel. The two possible modes of reactions are the $\text{He}^3(n,p)\text{T}$ charge-exchange reaction and the $\text{He}^3(n,d)\text{D}$ reaction. It is of interest to measure both reactions in view of the impact their results may have on our understanding of one of the simplest direct reactions available.

(3) Three- and four-body breakup reactions. These processes may yield information about the type of interactions in the final channel, and subsequently may give evidence for or against the existence of excited states in the trion system.

In a recent publication¹ an account of a measurement of the processes mentioned in case (3) was given. In this article we present the experimental results obtained by measuring the processes (1) and (2). No data are available for the elastic scattering reactions $\text{He}^3(n,p)\text{T}$ and $\text{He}^3(n,d)\text{D}$ in the 14-MeV region. Measurements of the inverse reactions $\text{D}(d,n)\text{He}^3$ and $\text{T}(p,n)\text{He}^3$ at charged-particle energies corresponding to $E_n \sim 14$ MeV in neutron-induced processes on He^3 are not known to the authors.

EXPERIMENTAL ARRANGEMENT

Neutrons of 14.4 MeV were obtained from the $\text{D}+\text{T}$ reaction using a 200-keV Cockcroft-Walton accelerator. The neutron flux of $1.5 \times 10^9 \text{ sec}^{-1}$ in 4π was monitored

by counting the associated α particles with a $\text{CsI}(\text{Tl})$ crystal 6 mg/cm² thick.

A schematic drawing of the experimental arrangement used in this experiment is shown in Fig. 1. Isotopically pure He^3 gas was contained in a gas cell 50 mm long, 16 mm in diam, lined with gold. The gas pressure in the He^3 target was 780 mm Hg (absolute). The gas cell was connected to a counter telescope through a Havar² foil 2.2 mg/cm² thick and 15 mm in diam.

The counter telescope consists of two proportional gas counters and a semiconductor silicon detector depleted to detect 15.2-MeV protons. The counters were filled with purified dry CO_2 to a pressure of 10 cm Hg. The pulses from the E and dE/dx counters were fed into a two-dimensional analyzer gated with a triple-coincidence pulse. After performing the two-dimensional analysis the $E\text{-}dE/dx$ data were displayed in a 100×100 array. The simultaneous detection either of proton, deuteron, and triton or He^3 and He^4 particle spectra was achieved by adjusting the high voltage applied to the proportional counters.

The energy resolution of the detecting system was 2% ($\Delta E = 300$ keV) for 15.0-MeV protons. The distance between the neutron source and the center of the He^3 target was 11.6 cm and that between the center of the He^3 target and the E detector was 15.5 cm. With such a geometry the angular resolution of the counter specified by the FWHM (full width at half-maximum) $\Delta\Theta$ of the window function amounts to 4.6° at a counter setting angle of 0° .

The absolute cross sections were determined by normalization to the elastic $n\text{-}p$ scattering. For this purpose the gas cell was filled with H_2 , purified through a palladium leak.

$\text{He}^3(n,n)\text{He}^3$

The recoil He^3 particles were detected to measure the scattering of neutrons in the backward direction. The experimental setup permitted the detection of He^3 particles in the range from 0° to 40° (lab). Beyond this range the energy of He^3 particles was below the counter threshold. The differential cross sections and the corresponding neutron scattering angles are tabulated in

¹ B. Antolković, M. Cerineo, G. Paić, P. Tomaš, V. Ajdačić, B. Lalović, W. T. H. Van Oers, and I. Slaus, *Phys. Letters* **23**, 477 (1966).

² Supplied by Hamilton Watch Company, Lancaster, Pennsylvania.

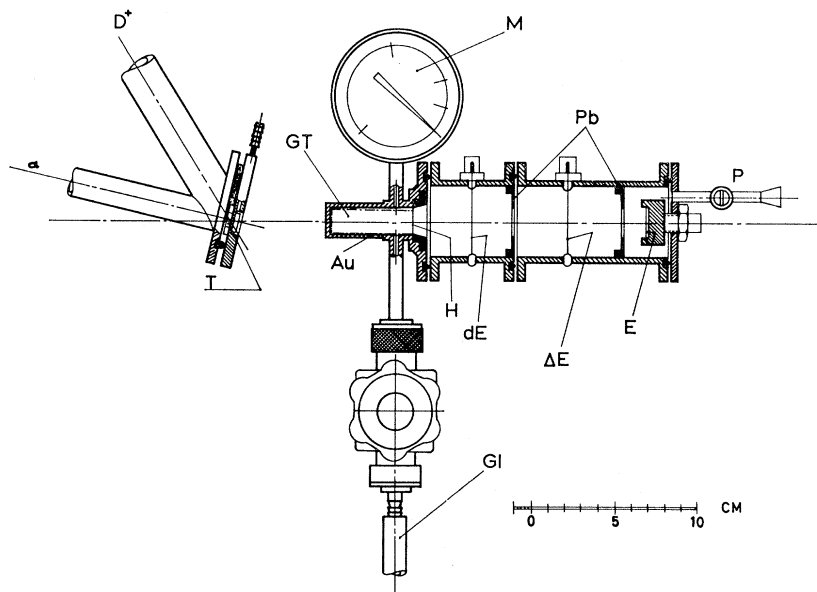


FIG. 1. A schematic drawing of the experimental arrangement: D^+ , incident deuteron beam; α , to the α -particle monitor; T, tritium target for the $D+T$ reaction; Au, gold lining; H, Havar foil; GI, He^3 gas inlet; GT, gas target; M, manometer; P, to the vacuum pump; Pb, lead diaphragms; dE , first proportional counter; ΔE , second proportional counter; E, semiconductor counter.

Table I. In Fig. 2 the experimental points are compared with the theoretical curves for the 14.0-MeV neutron energy given by Bransden, Robertson, and Swan.³ In the theoretical analysis used in Ref. 3 resonating-group wave functions were employed to obtain an integro-differential equation describing the collision. The He^3 wave function used was of the Gaussian type. The two-body interaction had exchange properties either of the Serber or of the symmetrical type and Gaussian radial dependence.

The experimental points are in agreement with the curve obtained by the symmetrical interaction. Actually, the experimental method used did not allow measurements of the lower-angular region, so the position of the minimum could not be determined. It should be said that the agreement in the backward part of the angular distribution cannot be taken as a strong indication toward the predominance of either type of interaction because at this energy and in the observed angular range the calculated angular distribution is not very sensitive to the type of forces used. It

TABLE I. Differential cross sections in the c.m. system for the $He^3(n,n)He^3$ reaction.

$\Theta_{c.m.}^0$	$d\sigma/d\Omega$ (mb/sr)
99.5	4.4 ± 4.2
109.0	5.3 ± 1.0
119.0	8.9 ± 1.0
129.0	18.1 ± 2.1
138.0	24.7 ± 1.0
148.0	37.9 ± 1.0
157.0	56.0 ± 1.0
167.0	70.0 ± 1.0

³ B. H. Bransden, H. H. Robertson, and P. Swan, Proc. Phys. Soc. (London) **A69**, 877 (1956).

remains as an imperative requirement that neutrons scattered at forward scattering angles should be measured in order to make possible a more substantial comparison with the theoretical calculations of Ref. 3.

$He^3(n,d)D$ and $He^3(n,p)T$

Angular Distributions

The differential cross sections measured for the $He^3(n,d)D$ and $He^3(n,p)T$ reactions in the present experiment are given numerically in Tables II and III. The corresponding angular distributions are plotted in Figs. 3 and 4. The large-angle data ($\Theta_{c.m.} > 82^\circ$) in the $He^3(n,p)T$ reaction were obtained by detecting the recoil tritons in the forward direction. Tables IV and V give the coefficients of the Legendre-polynomial analysis of the dashed curves in Figs. 3 and 4. The method developed by Showdon *et al.*⁴ was used for extracting

TABLE II. Differential cross sections in the c.m. system for the $He^3(n,d)D$ reaction.

$\Theta_{c.m.}^0$	$d\sigma/d\Omega$ (mb/sr)
8.45	39.6 ± 0.8
16.88	21.6 ± 0.7
25.29	14.5 ± 0.6
33.65	7.3 ± 0.6
41.95	0.7 ± 0.5
50.18	2.3 ± 0.5
58.31	3.4 ± 1.1
66.33	2.0 ± 0.6
74.20	4.7 ± 1.3
81.91	4.6 ± 1.4
96.70	0.8 ± 1.6
110.42	1.7 ± 1.7

⁴ S. C. Snowdon, L. Eisenbud, and J. F. Marschall, J. Appl. Phys. **29**, 950 (1958).

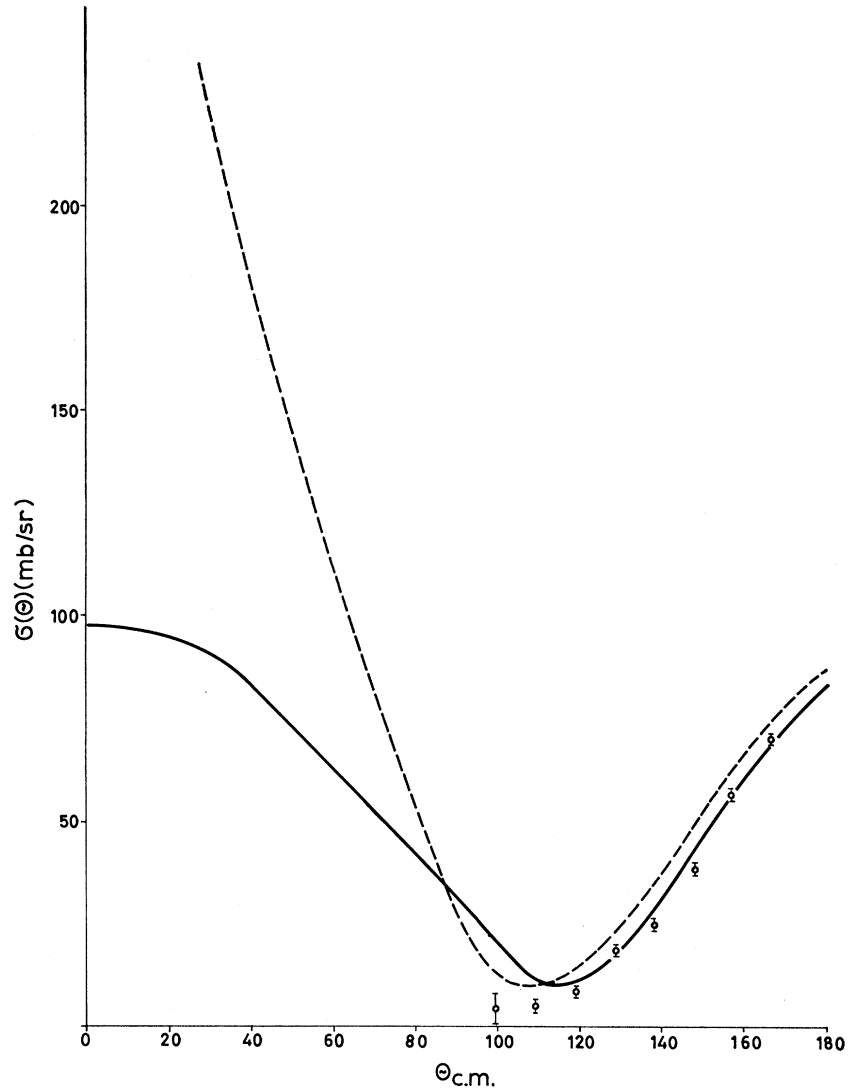


FIG. 2. The angular distribution of the He³(*n,n*)He³ reaction. The solid line is obtained using the symmetrical interaction. The dashed line is calculated by the Serber interaction. Both curves are calculated for $E_n=14.0$ MeV (see Ref. 3). The error bars on the experimental points indicate the statistical errors.

these coefficients of the Legendre polynomials in the expansion of the form

$$\sigma_{e.m.}(\Theta) = \sum_n A_n P_n(\cos\Theta).$$

By integration over Θ , the total cross sections were found to be 142.2 ± 6.3 mb and 66.4 ± 3.2 mb for the reactions He³(*n,p*)T and He³(*n,d*)D, respectively. The latter value is inferred from the fact that the angular distribution of the He³(*n,d*)D reaction is symmetrical with respect to 90° in the c.m. system. From these values the total cross sections for the inverse reactions can be easily computed. The values of 63.2 mb for the D(*d,n*)He³ and 133.0 mb for the T(*p,n*)He³ reaction at the corresponding energies $E_d=15.1$ MeV and $E_p=15.4$ MeV are obtained using the detailed balance theorem.

Discussion

In the theoretical analysis of the He³(*n,p*)T and He³(*n,d*)D reactions we assume that a direct mechanism

is involved, i.e., that no He⁴ excited-state formation takes part in the process. This assumption seems to be acceptable in view of the theoretical work of Selove⁵ and that of Young and Stein,⁶ claiming that the energy

TABLE III. Differential cross sections in the c.m. system for the He³(*n,p*)T reaction.

$\Theta_{c.m.}^0$	$d\sigma/d\Omega$ (mb/sr)	$\Theta_{c.m.}^0$	$d\sigma/d\Omega$ (mb/sr)
6.60	21.3 ± 1.2	91.7	6.5 ± 1.6
13.19	21.3 ± 1.2	101.4	5.5 ± 0.8
19.75	19.4 ± 0.8	111.2	5.5 ± 0.7
26.28	17.4 ± 1.2	121.0	6.0 ± 0.5
32.77	16.0 ± 1.4	130.8	9.1 ± 0.5
45.58	13.7 ± 2.0	140.6	13.4 ± 0.5
51.87	11.5 ± 1.6	150.5	18.4 ± 0.6
58.08	13.3 ± 3.0	160.3	26.0 ± 0.6
76.09	9.9 ± 3.3	173.4	35.4 ± 0.8
82.0	10.0 ± 1.7		

⁵ W. Selove, Phys. Rev. **103**, 136 (1956).

⁶ J. E. Young and P. R. Stein, Ann. Phys. (N. Y.) **15**, 157 (1961).

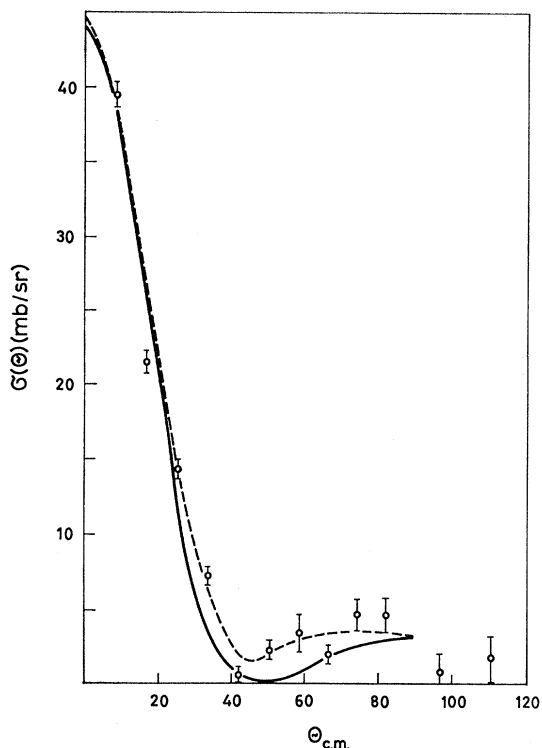


FIG. 3. The angular distribution of the $\text{He}^3(n,d)\text{D}$ reaction. The dashed line represents the curve obtained by the Legendre-polynomial expansion. The solid line is obtained by a PWBA treatment using a radius $r_0=4.5$ F. The error bars on the experimental points indicate the statistical errors.

dependence of the total cross sections can be explained without introducing the effects of He^4 excited states.

Within the framework of a direct-reaction mechanism the qualitative understanding of the processes is not very complex, although the quantitative theoretical treatment has not yet succeeded in giving unambiguous answers.

In the case of the $\text{He}^3(n,d)\text{D}$ reaction two modes of interaction can be considered. One is the simple proton pickup process, the other is governed by the interaction of the incident neutron with an n - p pair inside He^3 , giving rise to a knockout term. The experimental data were compared with the theoretical calculations of Van Oers and Brockman,⁷ who used a Born approximation in which the interference effects were taken into account. In the computations He^3 was represented by

TABLE IV. Coefficients of the Legendre-polynomial expansion fitted to the $\text{He}^3(n,d)\text{D}$ angular distribution.

n	A_n (mb/sr)	n	A_n (mb/sr)
0	5.83	6	10.51
2	12.36	8	1.30
4	15.25	10	-0.25

⁷ W. T. H. Van Oers and K. W. Brockman, Jr., Nucl. Phys. 48, 625 (1963).

the S part of the Pease and Feshbach wave function.⁸ The angular distribution obtained with an interaction radius of 4.5 F, plotted in Fig. 3, shows reasonable agreement in the small-angle region. The departure from the experimental points is more severe in the region from 25° to 90°, which is to be expected bearing in mind the shortcomings of the plane-wave Born approximation (PWBA).

Also, for the $\text{He}^3(n,p)\text{T}$ reaction two processes can be assumed to prevail. One of them is forward-peaked and results from the interaction between the incident neutron and the target proton. The other is due to the interaction between the incident particle and the remaining two nucleons in He^3 and may be called a heavy-particle stripping or core-exchange process giving rise to a large-angle peak in angular distributions.

The experimental data are compared with the calculations done by El Nadi and Rabie,⁹ using Gaussian trion wave functions, zero-range N - N potentials, and neglecting all kinds of distortions. This simple theory yields for the differential cross section a relation of the form

$$d\sigma/d\Omega \propto |A\bar{F} + B\bar{G}|^2, \quad (1)$$

where

$$\bar{F} = \exp(-K^2/16\gamma^2) \quad (2)$$

represents the knockout term.

$$\bar{G} = 4.489 \exp\left[-\frac{7q_2^2 + q_1^2}{56\gamma^2}\right] \quad (3)$$

is the heavy-particle stripping term, where

$$\mathbf{K} = \mathbf{q}_1 + \mathbf{q}_2 = \frac{2}{3}\mathbf{K}_p - \frac{2}{3}\mathbf{K}_n,$$

$$\mathbf{q}_1 = -\mathbf{K}_n - \frac{1}{3}\mathbf{K}_p,$$

$$\mathbf{q}_2 = \mathbf{K}_p + \frac{1}{3}\mathbf{K}_n.$$

\mathbf{K}_n and \mathbf{K}_p are the wave numbers of the incident neutron and the outgoing proton, respectively. For the parameter of the Gaussian wave function we assumed $\gamma^2=0.049$ F. As quoted by the authors, A and B are free-complex parameters.

The angular distribution obtained following these calculations using $|B|^2/|A|^2=0.2$ and taking the interference term $|AB^* + A^*B|/|A|^2$ to be $-\frac{2}{3}$ gives reasonable agreement with the data (see Fig. 4). It should be

TABLE V. Coefficients of the Legendre-polynomial expansion fitted to the $\text{He}^3(n,p)\text{T}$ angular distribution.

n	A_n (mb/sr)	n	A_n (mb/sr)
0	11.29	4	4.65
1	0.55	5	-0.21
2	11.31	6	1.95
3	-6.89	7	-1.68

⁸ R. L. Pease and H. Feshbach, Phys. Rev. 88, 945 (1952).

⁹ M. El Nadi and A. Rabie, Atomkernenergie 11, 233 (1966).

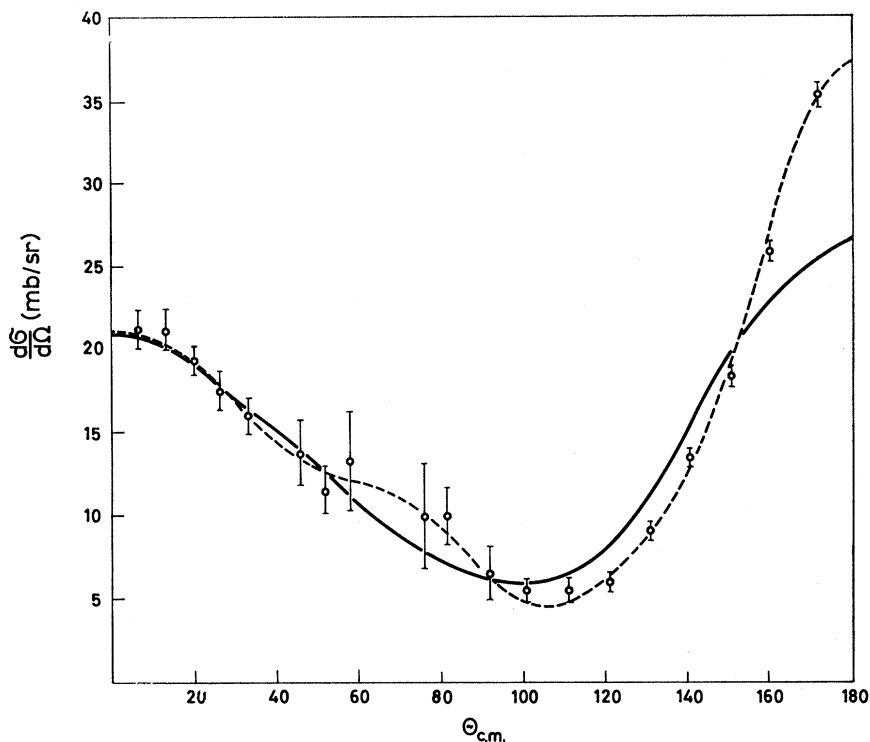


FIG. 4. The angular distribution of protons from the $\text{He}^3(n,p)\text{T}$ reaction. The solid line represents the curve obtained following the calculation in Ref. 9. The dashed line is calculated using the Legendre-polynomial expansion. The error bars on the experimental points indicate the statistical errors.

added that the $|B|^2/|A|^2$ value is reasonably well incorporated in the empirical energy dependence given for this ratio in Ref. 9. The $|B|^2/|A|^2$ ratio which gives the respective weight of the two processes involved tends to increase up to $E_p \approx 11$ MeV, at which point the ratio begins to decrease. That might be due to the advent of new types of mechanisms in this energy region. It is interesting to note that the turning point of the curve is approximately at the energy corresponding to the $\text{T}(p,n)\text{npp}$ threshold, which may be fortuitous, especially in the light of the bad fit achieved

at large angles, but can also indicate a substantial contribution of the total breakup process. It should be emphasized that the measurement of this reaction at higher energies is important and that it can be very useful for a better understanding of the mechanisms ruling the process.

ACKNOWLEDGMENTS

The authors wish to thank Dr. I. Šlaus for helpful discussions. It is a pleasure to thank Dr. P. Bornemisza for participating in the early stages of this experiment.